Acta Mech Sin (2010) 26:73–80
DOI 10.1007/s10409-009-0286-y

RESEARCH PAPER

Flow behavior in microchannel made of different materials with wall slip velocity and electro-viscous effects

Lei Wang · Jiankang Wu

Received: 23 February 2009 / Revised: 23 June 2009 / Accepted: 6 July 2009 / Published online: 31 October 2009

Abstract In a microfluidic system, flow slip velocity on a solid wall can be the same order of magnitude as the average velocity in a microchannel. The flow-electricity interaction in a complex microfluidic system subjected to joint action of wall slip and electro-viscous effect is an important topic. This paper presents an analytic solution of pressure-driven liquid flow velocity and flow-induced electric field in a two-dimensional microchannel made of different materials with wall slip and electro-viscous effects. The Poisson-Boltzmann equation and the Navier-Stokes equation are solved for the analytic solutions. The analytic solutions agree well with the numerical solutions. It was found that the wall slip amplifies the flow-induced electric field and enhances the electro-viscous effect on flow. Thus the electro-viscous effect can be significant in a relatively wide microchannel with relatively large κh, the ratio of channel width to thickness of electric double layer, in comparison with the channel without wall slip.

Keywords Microchannel · Wall slip · Electro-viscous effects

1 Introduction

In macroscopic flows, the non-slip boundary condition on a wall has been widely accepted. Although a number of recent studies [1–10] have found evidences of slip velocities for liquid flow over a hydrophobic wall (PDMS polymer materials), the wall slip velocity is generally very small in comparison with the average velocity in the macroscopic flow, and therefore it can been neglected. The wall slip velocity for liquid flow was first proposed by Navier in 1823, generally expressed as $u_s = \beta \partial u/\partial n$. $\partial u/\partial n$ is the normal derivative of velocity on walls, the parameter β is the slip length ranging from several micrometers to several microns, and it has been assumed to be a property parameter of wall material and working fluid. The contribution of wall slip velocity to mainstream velocity is the order of magnitude $0(\beta/h)$ [6], the ratio of slip length to flow scale (say channel width).

In microfluidic systems, the wall slip may play a significant role in flow-electricity interaction. A finite difference method was used to solve flow velocities in a rectangular microchannel with wall slip and electro-viscous effects [10]. Electrokinetic flows over inhomogeneously slipping surfaces was studied [11]. The wall slip can enhance electrokinetic effects [12]. Interfacially driven liquid transport can be amplified by hydrodynamic surface slip [13,14]. The effect of wall slip on electrokinetic energy conversion in a microfluidic system was examined [15,16] based on the classical Onsager relation [17]. In their studies the streaming potential is allowed to produce a net electric current through the microchannel, which was treated as an energy conversion device. The wall slip was found to enhance the electrokinetic conversion efficiency. In the cases of pressure driven flows in a microchannel with opened ends, the flow-induced streaming potential does not produce a net current in the microchannel, i.e., no energy conversion, but an electric resistance force retarding flow and reducing flow rate is generated. It is called electro-viscous effect [18–23]. The streaming potential is related to the pressure drop across the channel by the zero net current condition [20].

The project was supported by the National Natural Science Foundation of China (10872076).

L. Wang · J. Wu (✉)
Department of Mechanics,
Huazhong University of Science and Technology,
Wuhan National Laboratory of Optoelectronics,
430074 Wuhan, China
e-mail: wujkang@mail.hust.edu.cn

The flow behavior in a microchannel with either electro-viscous effect or wall slip has been well studied. The present study is focused on the combined effect of the wall slip and electro-viscosity on pressure driven flows in a microchannel. Polymer material PDMS has many advantageous optical, chemical and biological properties, and it is innocuous, easily fabricated and inexpensive. However, PDMS is a soft polymer material and can be easily deformed. A PDMS film is often attached onto glass substrate to be used. The flow behavior in a channel made of PDMS is different from that of the glass channel due to different surface properties. The slip flow occurs on PDMS surface due to low chemical energy and low attraction to liquid molecules [6–9]. Glass is a hydrophilic material and generally does not show surface slip velocity. Furthermore, the zeta electric potential on a PDMS surface is lower than that on a glass surface when contacted with electrolyte solution. This work tries to seek an analytic solution for the pressure-driven flows in a two-dimensional uniform microchannel made of PDMS and glass with wall slip and electro-viscous effects in order to gain a better understanding of the flow-electricity interaction in microfluidic systems. The steric effect may become significant as the size of channel goes down, or at large applied voltages [24,25]. The validity of P-B equation might be a question. However, it was pointed out in [24] that in the cases of surface potential 25–200 mV, sometimes called "weakly nonlinear regime", nonlinearity arises and the fundamental assumption of the ionic chemical potential, the Boltzmann distribution, remains valid.

2 Governing equations and boundary conditions

For the purpose of easy fabrication, slit-type microchannels are commonly used in microfluidic chips and their thickness is much less than their width, i.e., $H \ll W$. Upper layer of the microchannel is a PDMS film that is bonded on glass substrate. The flow in slit microchannel can be reasonably approximated as two-dimensional flows, as shown in Fig. 1.

In Fig. 1, H is the channel thickness. When a pressure gradient is applied across the channel, flow in x direction is generated. The following assumptions have been made in the present study:

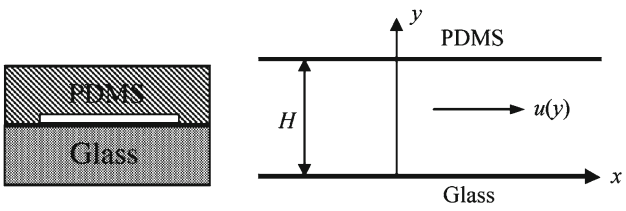

Fig. 1 A schematic representation of a two-dimensional microchannel

(1) The channel materials PDMS and glass are assumed to be complete insulated. The electric conductivity of wall will not be considered. The conductivity of bulk liquid is assumed to be a constant.
(2) The channel wall is uniformly flat, and the wall potentials are below the steric limit. The Poisson-Boltzmann equation is valid for describing of electric double layers.

Generally, body force except electric resistance can be ignored in a microfluidic system. The continuity equation and Navier-Stokes equation of steady flow for incompressible viscous fluid read:

$$\frac{\partial u}{\partial x} = 0, \tag{1}$$

$$-\frac{\mathrm{d}p}{\mathrm{d}x} + \mu\frac{\mathrm{d}^2u}{\mathrm{d}y^2} + \rho_e E_x = 0, \quad 0 \le y \le H, \tag{2}$$

where ρ_e is the volume charge density of fluid, E_x the flow-induced electric field. $\rho_e E_x$ the flow-induced electric resistance of per unit volume fluid. When wall slip occurs, the boundary conditions on the channel wall are specified as follows:

$$u = \beta_2\frac{\mathrm{d}u}{\mathrm{d}y}, \quad y = 0, \quad u = -\beta_1\frac{\mathrm{d}u}{\mathrm{d}y}, \quad y = H, \tag{3}$$

where β_1 and β_2 are the surface slip lengths of PDMS and glass, respectively. Surface slip length has been considered to be dependent on the properties of solid wall and liquid. For a symmetric electrolyte solution (1 : 1), the electric potential and charge density of electric double layers are governed by Poisson-Boltzmann equation (P-B):

$$\nabla^2\varphi = \frac{2n_0ze}{\varepsilon}\sinh\left(\frac{ze}{k_bT}\varphi\right), \tag{4}$$

$$\rho_e = -2n_0ze\sinh\left(\frac{ze}{k_bT}\varphi\right), \tag{5}$$

where ε and z are the dielectric constant and ionic valence of the solution, respectively; n_0 is the ionic number concentration of bulk fluid, e is the charge of a proton, k_b is the Boltzmann constant, and T is the absolute temperature. The boundary conditions of Eq. (4) on the wall are specified as follows:

$$\varphi = \zeta_2, \quad y = 0, \quad \varphi = \zeta_1, \quad y = H, \tag{6}$$

where ζ_1, ζ_2 are the wall Zeta potentials of PDMS and glass, respectively. Both wall slip velocity and electric double layers are tangent to the channel wall. It is assumed, in the present study, that the wall slip velocity does not interfere with the electric double layers, and the electric potential and charge density of electric double layers will not be changed in cases of wall slip in an infinite uniform microchannel. The flow-induced electric field is related to the flow velocity and governed by the electric current balance rule [11], which

states that the total current in the microchannel must be zero in a steady state, expressed as follows:

$$I_s + I_c = 0, \tag{7}$$

where I_s and I_c are the streaming current and the conductive current in a microchannel, respectively.

$$I_s = \int_0^H u\rho_e \mathrm{d}y, \tag{8}$$

$$I_c = \lambda_b E_x H, \tag{9}$$

where λ_b is the electric conductivity of bulk liquid. The relation of the electric field and the flow velocity is expressed as follows:

$$E_x = -\frac{I_s}{\lambda_b A} = -\frac{\int_0^H u\rho_e \mathrm{d}y}{\lambda_b H}. \tag{10}$$

The coupling equations (2), (4) and (10) with boundary conditions (3) and (6) are solved for flow velocity and flow-induced electric field in the microchannel. For generality, the flow variables are normalized to dimensionless forms:

$$\bar{x} = \frac{x}{H}, \quad \bar{y} = \frac{y}{H}, \quad \bar{u} = \frac{u}{U}, \quad \bar{p} = \frac{p}{\rho U^2}, \tag{11}$$

$$\bar{\varphi} = \frac{\varphi}{\zeta_0}, \quad \bar{\rho}_e = \frac{\rho_e}{(-\varepsilon\zeta_0/H^2)}, \quad \bar{E}_x = \frac{E_x}{(\varepsilon\zeta_0 U)/(\lambda_b H^2)}, \tag{12}$$

where the characteristic velocity $U = u_{\max} = -\frac{H^2}{8\mu}\frac{\mathrm{d}p}{\mathrm{d}x}$ is the maximum velocity in the microchannel without wall slip and electro-viscous effects, ζ_0 is the characteristic surface electric potential, λ_b and μ are the electric conductivity and the dynamic viscosity of the bulk liquid, and wall electric conductivity is neglected in the present study. Dimensionless P-B equation is expressed as

$$\bar{\nabla}^2\bar{\varphi} = \alpha_1 \sinh(\alpha_2\bar{\varphi}), \quad \bar{\rho}_e = \bar{\nabla}^2\bar{\varphi}, \tag{13}$$

where $\alpha_2 = \frac{ze\zeta_0}{K_b T}$ is a dimensionless parameter reflecting the property of EDL, and $\alpha_1 = (\kappa H)^2/\alpha_2$, κH is the ratio of channel thickness to the EDL thickness, $\kappa = \frac{1}{\lambda_D} = \sqrt{\frac{2n_0 z^2 e^2}{\varepsilon K_b T}}$, λ_D is the EDL thickness. The boundary conditions of Eq. (13) are given as

$$\bar{\varphi} = \zeta_2/\zeta_0, \quad \bar{y} = 0, \quad \bar{\varphi} = \zeta_1/\zeta_0, \quad \bar{y} = 1. \tag{14}$$

Equation (13) can be solved for charge density by finite difference and iterative algorithm without difficulties. Dimensionless form of the flow Eq. (2) is written as follows:

$$\frac{\mathrm{d}^2\bar{u}}{\mathrm{d}\bar{y}^2} = Re\frac{\mathrm{d}\bar{p}}{\mathrm{d}\bar{x}} + \gamma\bar{\rho}_e\bar{E}_x = F(\bar{y}), \quad 0 \le \bar{y} \le 1, \tag{15}$$

where $Re = \rho U H/\mu$ is Reynolds number, $\gamma = (\varepsilon\zeta_0)^2/(\mu\lambda_b H^2)$ is defined as electro-viscous number reflecting the ratio of flow-induced electric resistance to viscous force. The dimensionless boundary conditions are written as

$$\bar{u} = \frac{\beta_2}{H}\frac{\mathrm{d}\bar{u}}{\mathrm{d}\bar{y}}, \quad \bar{y} = 0, \quad \bar{u} = -\frac{\beta_1}{H}\frac{\mathrm{d}\bar{u}}{\mathrm{d}\bar{y}}, \quad \bar{y} = 1. \tag{16}$$

Dimensionless form of the electric field Eq. (10) is written as follows:

$$\bar{E}_x = \int_0^1 \bar{u}\bar{\rho}_e \mathrm{d}\bar{y}. \tag{17}$$

3 Analytic solution of a two-dimensional microchannel with wall slip and electro-viscous effects

For the analytic solution of flow Eq. (15), introduce an equation

$$\frac{\mathrm{d}^2\bar{u}}{\mathrm{d}\bar{y}^2} = c\bar{u}, \tag{18}$$

where c is a constant to be determined. The solutions of Eq. (18) can be expanded as an infinite series of eigenfunctions $Y_m(\bar{y})$

$$\bar{u}(\bar{y}) = \sum_{m=1}^{\infty} \bar{u}_m Y_m(\bar{y}). \tag{19}$$

The general solutions of the eigenfunctions can be expressed as

$$Y_m(\bar{y}) = c_1\cos(\lambda_m\bar{y}) + c_2\sin(\lambda_m\bar{y}). \tag{20}$$

The first order derivative of the eigenfunctions is written as

$$Y_m'(\bar{y}) = -c_1\lambda_m\sin(\lambda_m\bar{y}) + c_2\lambda_m\cos(\lambda_m\bar{y}). \tag{21}$$

Making use of the boundary condition (16), one obtains

$$c_1 = \frac{c_2\lambda_m\beta_2}{H}, \tag{22}$$

$$c_1\cos(\lambda_m) + c_2\sin(\lambda_m) = -\frac{\beta_1}{H}(-c_1\lambda_m\sin(\lambda_m) + c_2\lambda_m\cos(\lambda_m)). \tag{23}$$

Substituting Eq. (22) into Eq. (23), an algebraic equation for eigenvalues λ_m is obtained

$$\mathrm{tg}(\lambda_m) = \frac{(\beta_1+\beta_2)\lambda_m H}{\beta_1\beta_2\lambda_m^2 - H^2}. \tag{24}$$

The eigenvalues $\lambda_1, \lambda_2, \lambda_3, \ldots, \lambda_m, \ldots$ can be solved by using Newton iterative algorithm (see Appendix A). So the eigenfunctions are expressed as follows:

$$Y_m(\bar{y}) = \frac{c_2\beta_2\lambda_m}{H}\cos(\lambda_m\bar{y}) + c_2\sin(\lambda_m\bar{y}) = c_2\left[\frac{\beta_2\lambda_m}{H}\cos(\lambda_m\bar{y}) + \sin(\lambda_m\bar{y})\right]. \tag{25}$$

The nonslip condition on the glass surface ($\beta_2 = 0$) yields

$$Y_m(\bar{y}) = \sin(\lambda_m \bar{y}). \tag{26}$$

Substituting Eq. (26) into Eq. (19), one has

$$\sum_{m=1}^{\infty} \frac{\mathrm{d}^2 Y_m(\bar{y})}{\mathrm{d}\bar{y}^2} = \sum_{m=1}^{\infty} c_m Y_m(\bar{y}). \tag{27}$$

Substituting Eq. (27) into Eq. (18) obtains

$$c_m = -\lambda_m^2. \tag{28}$$

The forcing function $F(\bar{y})$ of Eq. (15) is expanded as an infinite series of eigenfunctions $Y_m(\bar{y})$

$$F(\bar{y}) = \sum_{m=1}^{\infty} f_m Y_m(\bar{y}). \tag{29}$$

Substituting Eqs. (26) and (29) into Eq. (15) yields

$$\sum_{m=1}^{\infty} \bar{u}_m \frac{\mathrm{d}^2 Y_m}{\mathrm{d}\bar{y}^2} = \sum_{m=1}^{\infty} c_m \bar{u}_m Y_m = \sum_{m=1}^{\infty} f_m Y_m. \tag{30}$$

So we have

$$\bar{u}_m = \frac{f_m}{c_m}. \tag{31}$$

Making use of orthogonality of the eigenfunctions

$$\int_0^1 Y_m Y_{m'} \mathrm{d}y = 0, \quad \text{for} \quad m \neq m'.$$

One obtains

$$f_m = \frac{\int_0^1 F(\bar{y}) Y_m(\bar{y}) \mathrm{d}\bar{y}}{\int_0^1 Y_m(\bar{y}) Y_m(\bar{y}) \mathrm{d}\bar{y}} = \frac{f_m^{(1)}}{f_m^{(2)}}. \tag{32}$$

Substituting Eqs. (31) and (32) into Eq. (12) yields

$$\begin{aligned} f_m^{(1)} &= \frac{\rho U H}{\mu} \frac{\partial \bar{p}}{\partial \bar{x}} \int_0^1 Y_m \mathrm{d}\bar{y} + \bar{E}_x \frac{\varepsilon^2 \zeta^2}{\mu \lambda_b H^2} \int_0^1 \bar{\rho}_e Y_m \mathrm{d}\bar{y} \\ &= \frac{\rho U H}{\mu} \frac{\partial \bar{p}}{\partial \bar{x}} \left(-\frac{1}{\lambda_m} \cos(\lambda_m) + \frac{1}{\lambda_m} \right) \\ &\quad + \bar{E}_x \frac{\varepsilon^2 \zeta^2}{\mu \lambda_b H^2} \int_0^1 \bar{\rho}_e Y_m \mathrm{d}\bar{y}, \end{aligned} \tag{33}$$

$$f_m^{(2)} = \int_0^1 Y_m Y_m \mathrm{d}\bar{y} = \frac{1}{2} - \frac{1}{4\lambda_m} \sin(2\lambda_m). \tag{34}$$

Dimensionless equation of electric field (10) is rewritten as

$$\bar{E}_x = \int_0^1 \bar{u} \bar{\rho}_e \mathrm{d}\bar{y} = \sum_{m=1}^{\infty} \bar{u}_m \int_0^1 \bar{\rho}_e Y_m \mathrm{d}\bar{y}. \tag{35}$$

Substituting Eqs. (31)–(34) into Eq. (35) yields

$$\bar{E}_x = \sum_{m=1}^{\infty} D_m \Big/ \left(1 - \sum_{m=1}^{\infty} G_m \right), \tag{36}$$

where

$$D_m = \frac{Re}{c_m f_m^{(2)}} \frac{\partial \bar{p}}{\partial \bar{x}} \left(-\frac{1}{\lambda_m} \cos(\lambda_m) + \frac{1}{\lambda_m} \right) \int_0^1 \bar{\rho}_e Y_m \mathrm{d}\bar{y}, \tag{37}$$

$$G_m = \frac{\gamma \left(\int_0^1 \bar{\rho}_e Y_m \mathrm{d}\bar{y} \right)^2}{c_m f_m^{(2)}}. \tag{38}$$

4 A typical example and disscuson

According to [20], typical parameters of electrokinetic flow in a microchannel are the following:

channel thickness	$H = 3\ \mu\mathrm{m}$,
characteristic velocity	$U = 0.01\ \mathrm{m/s}$,
corresponding pressure gradient	$\frac{\mathrm{d}p}{\mathrm{d}x} = 0.88 \times 10^7\ \mathrm{Pa \cdot s^{-1}}$,
dimensional pressure gradient	$\frac{\mathrm{d}\bar{p}}{\mathrm{d}\bar{x}} = \frac{H}{\rho U^2} \frac{\mathrm{d}p}{\mathrm{d}x} = -266$,
density	$\rho = 1{,}000\ \mathrm{kg \cdot m^{-3}}$,
dynamic viscosity	$\mu = 0.9 \times 10^3\ \mathrm{Ns \cdot m^{-2}}$,
electric conductivity of liquid	$\lambda_b = 1.468719 \times 10^{-4}\ \Omega^{-1}\mathrm{m}^{-1}$,
dielectric constant in vacuum	$\varepsilon_0 = 8.854 \times 10^{-12}\ \mathrm{C^2 N^{-1} m^{-2}}$,
relative dielectric constant of liquid	$\varepsilon_r = 78.5$,
Boltzmann constant	$K_b = 1.38 \times 10^{-23}\ \mathrm{J/K}$
absolute temperature	
ionic number concentration of bulk solution	$T = 298\ \mathrm{K}$, $n_0 = 7.28662 \times 10^{21}$,
Zeta potential on glass surface	$\zeta_2 = -100\ \mathrm{mV}$,
Zeta potential on PDMS surface	$\zeta_1 = -50\ \mathrm{mV}$,
characteristic surface potential	$\zeta_0 = -50\ \mathrm{mV}$,
EDL parameter	$\kappa H = 35$,
surface slip length of PDMS	$\alpha_2 = -1.95$,
dimensionless slip length	$\bar{\beta} = \beta_1 / H = 0.03$, $\bar{\beta}_2 = 0$.

There is no slip on glass surface, and the electro-viscous number $\gamma = 0.0, 0.03$. The velocity profile in a channel section are shown in Figs. 2 and 3. The numerical solutions are also given for a comparison.

It can be seen that the slip velocity on the PDMS wall ($\bar{y} = 1$) is about 0.1 times that of the maximum velocity in the present case. The overall flow velocity in a microchannel increases due to the wall slip. The maximum velocity increases to about 1.05 times that of the corresponding velocity when there is no wall slip, as shown in Fig. 1 ($\bar{\beta} = 0.03$, $\gamma = 0$). Meanwhile, it is found that the electro-viscous effect decreases the flow velocity in a microchannel as shown in Fig. 3 ($\bar{\beta} = 0$, $\gamma = 0.03$). The velocity profile in a channel section with varying slip lengths is shown in Fig. 4, where $\bar{\beta} = 0.03, 0.06, 0.09$, and $\gamma = 0.03$.

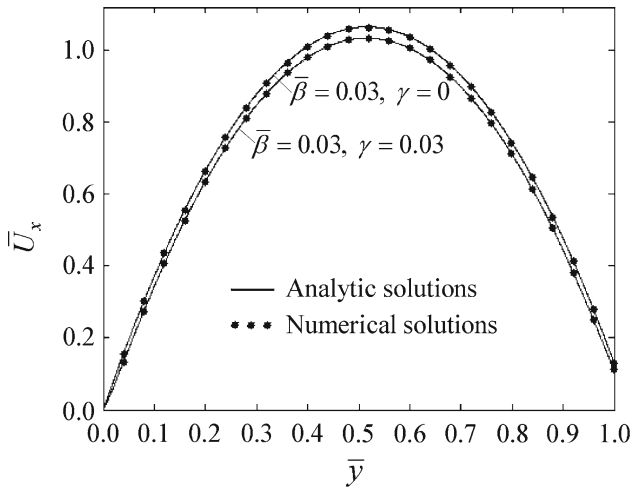

Fig. 2 Flow velocity profile in a channel section with electro-viscous effect and wall slip

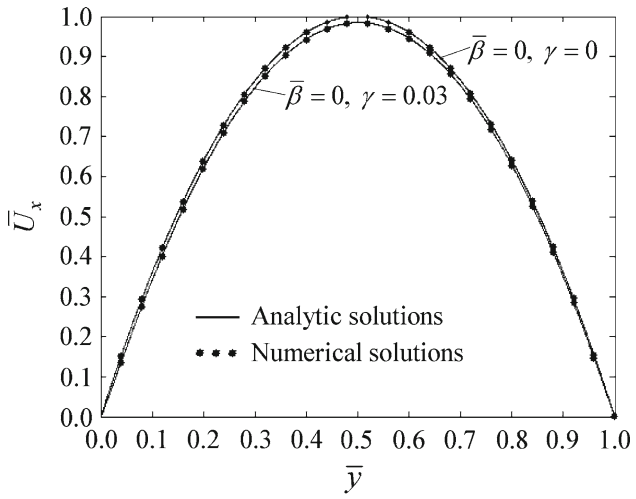

Fig. 3 Flow velocity profile in a channel section with electro-viscous effects, but without wall slip

It can be seen that the flow velocity in a microchannel increases with wall slip lengths. The slip velocity on the PDMS wall also increases with slip lengths, as shown in Fig. 5.

It is found that the wall slip velocity increases linearly with the slip length when there are no electro-viscous effects, and increases non-linearly when there are electro-viscous effects. The flow-induced electric field is one of the important phenomena of flow-electricity interaction in a microfluidic system. In the present example the flow-induced electric field with varying slip lengths is shown in Fig. 6.

It is interesting to find that the wall slip amplifies the flow-induced electric field when other parameters are fixed. With the fixed pressure gradient, the wall slip increases the overall flow velocity in a microchannel, and results in an increase of streaming current. Thus the flow-induced electric

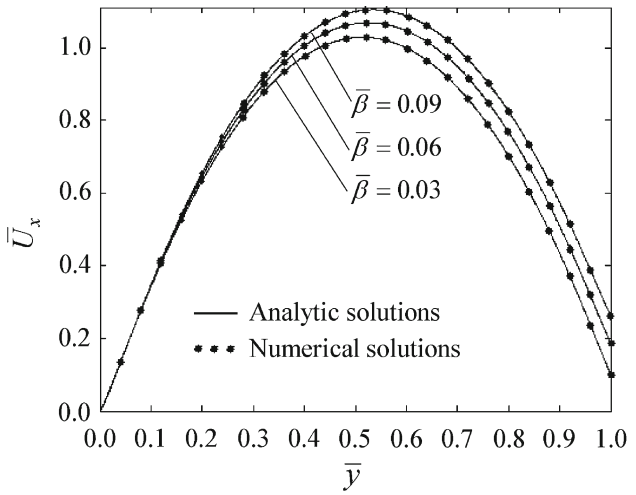

Fig. 4 Velocity profile in a microchannel with varying wall slip lengths, $\gamma = 0.03$

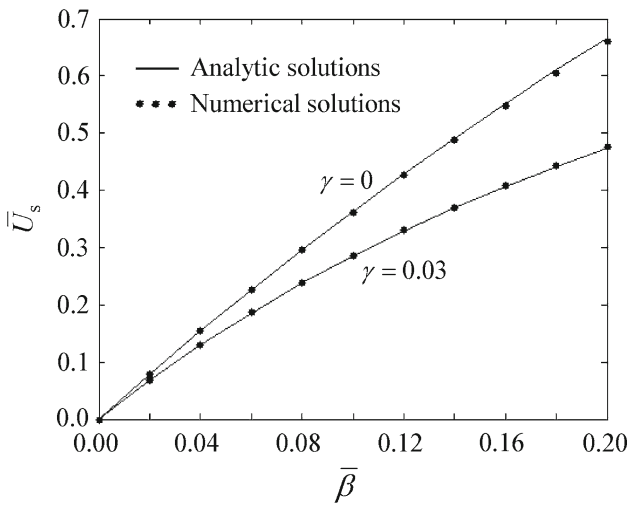

Fig. 5 Slip velocity on PDMS wall versus surface slip lengths

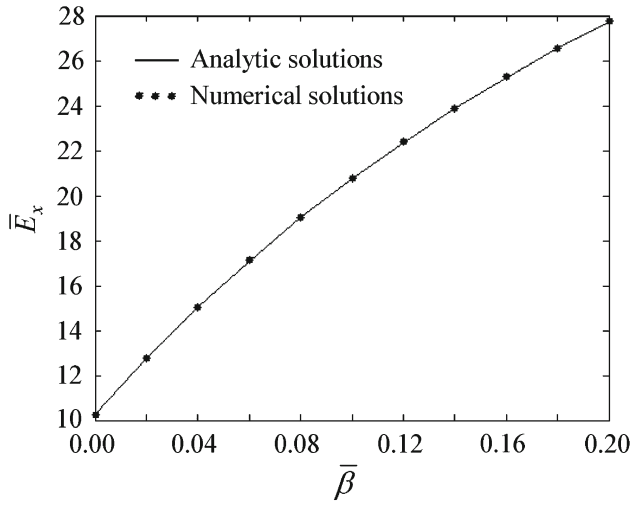

Fig. 6 Flow-induced electric fields versus wall slip lengths, when $\gamma = 0.03$

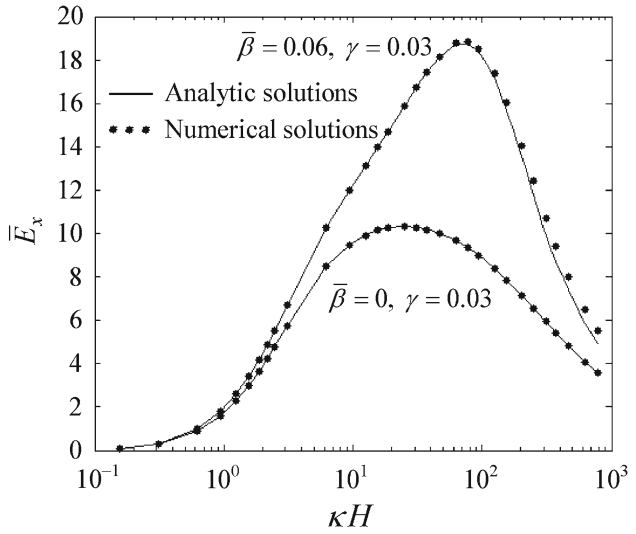

Fig. 7 Flow-induced electric fields versus κH values

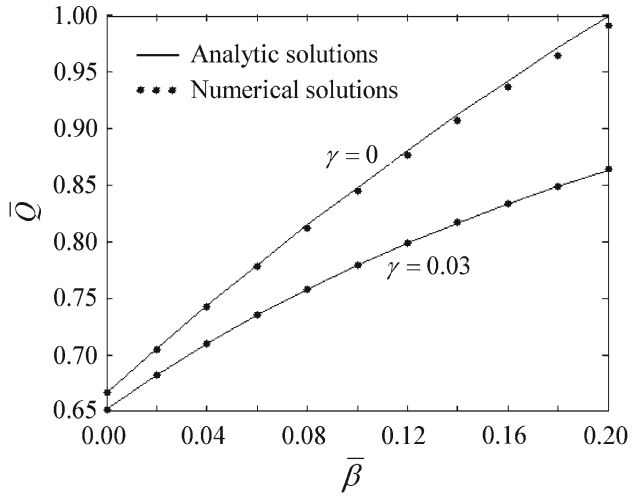

Fig. 8 Flow rates in a microchannel versus wall slip lengths

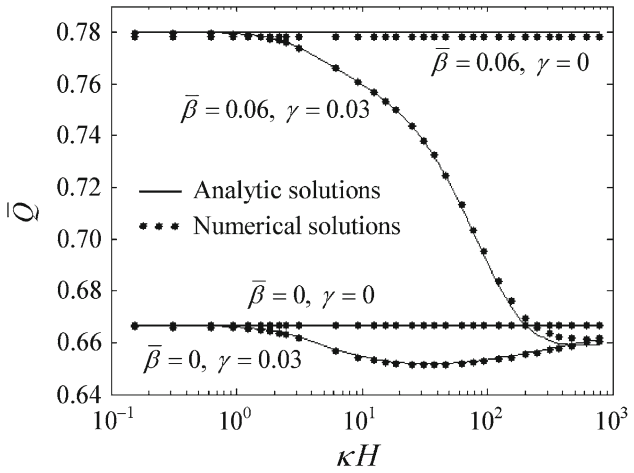

Fig. 9 Flow rates of microchannel versus κH values

field increases, see Eqs. (8)–(10). In the current example, the flow-induced electric fields with slip lengths $\bar{\beta} = 0.1, 0.2$ are approximately two times and three times that of those when there is no slip ($\bar{\beta} = 0$), respectively. It is also found that the flow-induced electric field varies significantly with κH values, the ratio of the channel thickness to the EDL thickness. The relationship of electric field and κH is shown in Fig. 7.

It is shown that the flow-induced electric field reaches the maximum in the region of κH value. The electric field reaches the maximum in the region $20 < \kappa H < 40$ when there is no wall slip $\bar{\beta} = 0.0$ in the present example. The electric field reaches the maximum in the region $80 < \kappa H < 100$ when the wall slip length $\bar{\beta} = 0.06$. A large κH implies that the electric double layers are very thin relative to the channel width, and therefore the electro-viscous effect of electric double layers on the bulk fluid are trivial. A small κH implies that the channel width is very small and the velocity in a microchannel is very small with fixed pressure gradient, $\bar{u} \sim 0(h^2)$. The streaming current is also small and therefore the flow-induced electric field and electro-viscous effect are less significant. The flow rate in a microchannel increases with the increase of wall slip lengths, as shown in Fig. 8.

It can be seen that the wall slippage increases the flow rate and the electro-viscous effect decreases the flow rate. The relationship of the flow rate in a microchannel and κH value is shown in Fig. 9.

As shown, when the electro-viscous effect ($\gamma = 0$) is ignored, the flow rate is independent of κH value, no matter there is a wall slip or not. When the electro-viscous effect is taken into consideration ($\gamma = 0.03$), the electro-viscous effect plays a significant role in the flow rate. The minimum flow rate (corresponding to the maximum electro-viscous effect) appears around $\kappa H \approx 30$ for a non-slip wall

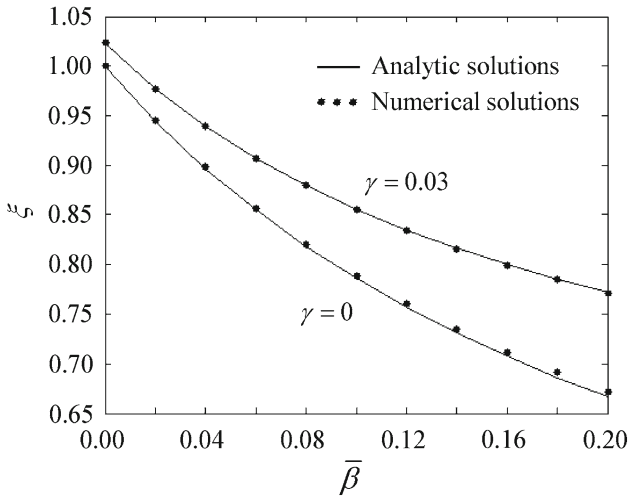

Fig. 10 The viscosity ratios versus wall slip lengths

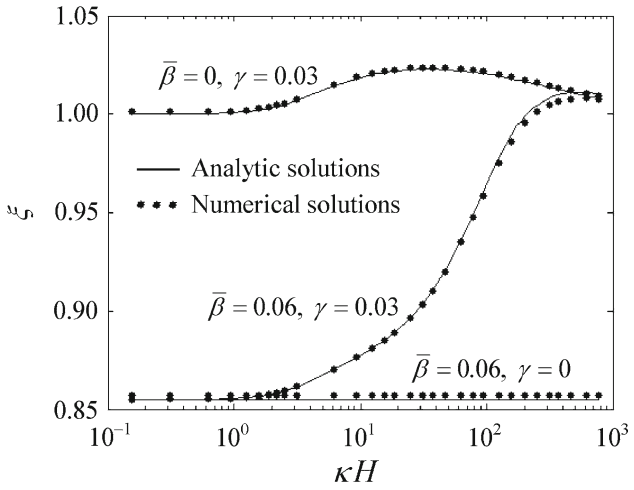

Fig. 11 The viscosity ratios versus κH values

($\bar{\beta} = 0.0$), and around $\kappa H \approx 500$ for a slip wall ($\bar{\beta} = 0.06$). It is also found that the electro-viscous effect is much greater in slip wall cases than that in non-slip wall cases. It implies that the wall slip velocity amplifies the electro-viscous effect on flow, and the κH region of minimum flow rate has been shifted to a higher value of κH. Therefore, the electro-viscous effect can also be significant in a wider microchannel with the wall slip ($\kappa H \approx 500$, in the present case). For a non-slip wall, the electro-viscous effect is important only in a narrow microchannel ($\kappa H \approx 30$ in the present case).

The electro-viscous effect decreases the flow rate in a microchannel, as if the fluid has a higher apparent viscosity. The ratio of apparent viscosity to physical viscosity of fluid is an indicator of the electro-viscous effect in a microchannel. A viscosity ratio is defined as $\xi = \mu/\mu_0$, where μ and μ_0 are the physical viscosity and the apparent viscosity, respectively. The viscosity ratio with varying wall slip lengths is shown in Fig. 10.

It can be seen that the wall slip decreases the viscosity ratio, no matter the electro-viscous effect is taken into consideration or not. The viscosity ratio with varying κH values is shown in Fig. 11. It shows that the viscosity ratio is independent of κH values when the electro-viscous effect is ignored. When the electro-viscous effect is taken into consideration, the viscosity ratio reaches the maximum around $\kappa H \approx 30$ for a non-slip wall ($\bar{\beta} = 0.0$ in the present case), and around $\kappa H \approx 500$ for a slip wall ($\bar{\beta} = 0.06$ in the present case).

5 Conclusion remark

The pressure-driven flow behavior in a two-dimensional uniform microchannel made of PDMS and glass was studied in this work. The combined effects of the wall slip and electro-viscosity on flows were taken into consideration. An analytic solution was reported and in good agreement with numerical solutions. The wall slip increases the flow velocity, and the electro-viscous effect of electric double layers decrease the flow velocity and the flow rate in a microchannel. The wall slip amplifies the flow-induced electric field and enhances the electro-viscous effect on flows. Therefore, the electro-viscous effect can be significant in a relatively wide microchannel with a relatively large ratio of microchannel width and thickness of electric double layers. The electro-viscous effect on flows is trivial when the ratio of the channel width to the thickness of electric double layers is either very large or very small.

Appendix A

Eigenvalue Eq. (24) $\mathrm{tg}(\lambda_m) = \frac{(\beta_1+\beta_2)\lambda_m H}{\beta_1\beta_2\lambda_m^2 - H^2}$ can be reduced to $\mathrm{tg}(\lambda_m) = -\frac{\beta_1}{H}\lambda_m$, when $\beta_2 = 0$ (non-slip on glass wall), as shown in Fig. 12. Eigenvalues λ_m can be solved by Newtonian iterative algorithm. Follows are initial values $\lambda_1^{(0)} = \pi/2$, $\lambda_m^{(0)} = \lambda_{m-1} + \pi$.

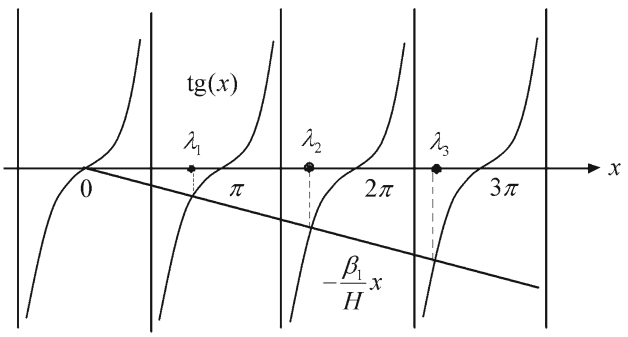

Fig. 12 Sketch of the numerical solutions of eigenvalues λ_m

References

1. Baudry, J., Charlaix, E., Tonck, A., Mazuyer, D.: Experimental evidence for a large slip effect at a non-wetting fluid-solid interface. Langmui **17**, 5232–5236 (2001)
2. Pit, R., Hervet, H., Léger, L.: Direct experimental evidence of slip in hexadecane: solid interfaces. Phys. Rev. Lett. **85**(5), 980–983 (2000)
3. Pit, R., Hervet, H., L'eger, L.: Friction and slip of a simple liquid at a solid surface. Tribol. Lett. **7**, 147–152 (1999)
4. Zhu, Y.X., Granick, S.: Limits of the hydrodynamic no-slip boundary condition. Phys. Rev. Lett. **88**(11), 106102 (2002)
5. Barrat, J.L.: Large slip effect at a non-wetting fluid-solid interface. Phys. Rev. Lett. **82**, 4671–4674 (1999)
6. Tretheway, D.C., Meinhart, C.D.: Apparent fluid slip at hydrophobic microchannel walls. Phys. Fluids **14**(3), L9–L12 (2002)
7. Ou, J., Perot, B., Rothstein, J.P.: Laminar drag reduction in microchannels using ultrahydrophobic surfaces. Phys. Fluids **16**(12), 4635–4643 (2004)
8. Tretheway, D.C., Meinhart, C.D.: A generating mechanism for apparent fluid slip in hydrophobic microchannels. Phys. Fluids **16**(5), 1509–1515 (2004)
9. Joseph, P., Tabeling, P.: Direct measurement of the apparent slip length. Phys. Rev. E **71**, 035303(R) (2005)
10. Chun, M.S., Lee, T.S., Lee, K.: Microflow of dilute colloidal suspension in narrow channel of microfluidic-chip under Newtonian fluid slip condition. K. Aust. Rheol. J. **17**(4), 207–215 (2005)
11. Squires T.M.: Electrokinetic flows over inhomogeneously slipping surfaces. Phys. Fluids **20**(9), 092105 (2008)
12. Muller, V.M., Sergeeva, I.P., Sobolev, V.D., Churaev, N.V.: Boundary efects in the theory of electrokinetic phenomena. Colloid J. USSR **48**, 606–614 (1986)
13. Ajdari, A., Bocquet, L.: Giant amplification of interfacially driven transport by hydrodynamic slip: Diffusio-osmosis and beyond. Phys. Rev. Lett. **96**(18), 186102 (2006)
14. Bazant, M.Z., Vinogradova, O.I.: Tensorial hydrodynamic slip. J. Fluid Mech. **613**, 125–134 (2008)
15. Davidson, C., Xuan, X.C.: Electrokinetic energy conversion in slip microchannels. J. Power Sour. **179**, 297–300 (2008)
16. Ren, Y.Q., Stein, D.: Slip-enhanced electrokinetic energy conversion in microfluidic channels. Microtechnology **19**, 195707 (2008)
17. Brunet, E., Ajdari, A.: Generalized Onsager relations for electrokinetic effects in anisotropic and heterogeneous geometries. Phys. Rev. E **69**, 016306 (2004)
18. Hunter, R.J.: Zeta Potential in Colloidal Science, Principle and Application. Academic Press, New York (1981)
19. Lyklema, J.: Fundamentals of Interface and Colloidal Science, vol. II. Academic Press, New York (1995)
20. Li, D.Q.: Electrokinetics in Microfluidics. Elsevier Academic Press, New York (2004)
21. Yang, C., Li, D.Q., Masliyah, J.H.: Modeling forced liquid convection in rectangular microchannels with electrokinetic effects. Int. J. Heat Mass Transf. **41**, 4229–4249 (1998)
22. Ren, L.Q., Qu, W.L., Li, D.Q.: Interfacial electrokinetic effects on liquid flow in microchannels. Int. J. Heat Mass Transf. **44**, 3125–3134 (2001)
23. Chun, M.S., Lee, S.Y., Yang, S.M.: Estimation of Zeta-potential by electrokinetic analysis of ionic fluid flows through a divergent microchannel. J. Colloid Interface Sci **266**, 120–126 (2003)
24. Kilic, M.S., Bazant, M.Z., Ajdari, A.: Steric effects in the dynamics of electrolytes at large applied voltages. I. Double-layer charging. Phys. Rev. E **75**, 021502 (2007)
25. Kilic, M.S., Bazant, M.Z., Ajdari, A.: Steric effects in the dynamics of electrolytes at large applied voltages. II. Modified Poisson-Nernst-Planck equations. Phys. Rev. E **75**, 021503 (2007)